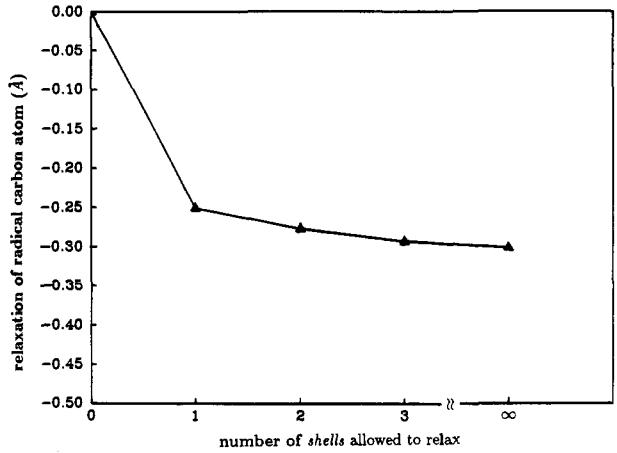

Figure 4. Same as Figure 3 except that the vertical relaxation distance of the radical carbon atom instead of relaxation energy is now plotted against the number of shells of carbon atoms allowed to relax.

three carbon atoms, etc. Figure 4 is the corresponding plot for the pyramidalization about the radical center.

Although the absolute magnitude of the energetic and structural effects of radical relaxation is about 50% larger for the empirical potential, the results are consistent with the ab initio calculations in that most of he energetic and structural effects of radical relaxation result from motion of only the radical carbon atom itself. The effect converges rapidly after the first carbon atom and collectively contributes only about another 10–15% to the radical relaxation.

VII. Conclusions

The radical generated by removing a hydrogen atom from hydrogenated diamond {111} is able, despite the constraints imposed by the surrounding lattice, to relax nearly to the extent that it does in the gas phase. This, in part, is because the radical is willing to accept shorter CC bond lengths and can therefore sink down toward planarity without disturbing the surrounding lattice. Thus bond strengths to surface carbon atoms should be similar to (about 1 kcal/mol greater than) bond strengths to gas-phase tertiary carbon atoms. Furthermore, this analysis holds for the transition states for abstraction reactions as well; the constraints of the lattice have little effect on the barriers for hydrogen abstraction reactions. We calculate an increase in the activation energy of only 0.2 kcal/mol when the structure surrounding a tertiary carbon atom is constrained similar to the way it is in a diamond lattice as compared to an unconstrained gas-phase reaction. Therefore, in kinetic modeling or molecular dynamics simulations of diamond film growth, the use of activation energies for surface hydrogen abstraction reactions taken from analogous gas-phase hydrocarbon reactions with minimal or no adjustment is justified.

Acknowledgment. This research was supported by the Office of Naval Research through the Naval Research Laboratory.

Registry No. H_2, 12385-13-6; $(CH_3)_3CH$, 75-28-5; diamond, 7782-40-3.

Heteronuclear Diatomic Metal Cluster Ions in the Gas Phase: Theoretical Treatment of $MgFe^+$ and Study of Its Reactions with Hydrocarbons

Lisa M. Roth,[†] Ben S. Freiser,*[,†] Charles W. Bauschlicher, Jr.,[‡] Harry Partridge,[‡] and Stephen R. Langhoff[‡]

Contribution from the Department of Chemistry, Purdue University, West Lafayette, Indiana 47907, and NASA Ames Research Center, Moffett Field, California 94035.
Received July 2, 1990. Revised Manuscript Received October 29, 1990

Abstract: The unique reactivity of $MgFe^+$ is described. This cluster reacts with linear alkenes (C_2–C_6) by displacement of magnesium to form an Fe^+–olefin product. In contrast, $MgFe^+$ reacts with alcohols by displacement of the iron to form a Mg^+–alcohol product. This is the first example of a changeover in the relative metal–ligand bond energies with both metals in a dimer being selectively displaced. $MgFe^+$ also reacts with cyclic alkenes. For example, it dehydrogenates cyclohexene to form $MgFe^+$–benzene, which reacts further to displace the magnesium and form benzene–Fe^+–cyclohexene. $MgFe^+$ is unreactive with small alkanes (C_2–C_4) but reacts with larger alkanes (C_5–C_7) to form a $MgFe^+$–alkene product. An upper limit of 34 ± 5 kcal/mol for $D°(Mg^+–Fe)$ has been established by use of ion–molecule reactions. In contrast, the photodissociation threshold for $MgFe^+$ to form Fe^+ yields an upper limit of $D°(Mg^+–Fe) \leq 44 \pm 3$ kcal/mol. Theoretical calculations show that $MgFe^+$ has a $X^6\Delta$ ground state and bonds by forming a covalent Fe(4s)–Mg(3s) bond. The computed binding energy of 29.4 kcal/mol, which is expected to be a lower bound, is consistent with the upper limit determined from ion–molecule reactions. The calculations show that the photon absorption at ≃49 kcal/mol corresponds to the intense $(2)^6\Delta \leftarrow X^6\Delta$ transition. This explains the large difference between the dissociation energy deduced from the ion–molecule reactions and the upper bound determined from photodissociation.

Introduction

The gas-phase chemistry of atomic metal ions and small metal cluster ions continues to be of great interest.[1] These systems provide information that can be applied to a wide range of disciplines, including surface science, catalysis, and atmospheric chemistry. For example, magnesium and iron have been detected in the atmosphere by airborne mass spectrometers. These metals are introduced by meteor ablation and have been observed in the 100-km-altitude region.[2] Several laboratory studies have been

[†] Purdue University.
[‡] NASA Ames Research Center.

(1) Morse, M. D. *Chem. Rev.* **1986**, *86*, 1049.

0002-7863/91/1513-3274$02.50/0

completed concerning the atomic metal ions Mg^+[3] and Fe^+[4] and the mixed-metal dimer species MFe^+ (M = transition metal). The present work extends this by characterizing the heteronuclear diatomic ion $MgFe^+$. This is also the first report of a heteronuclear diatomic ion that is composed of both a transition metal and a main-group metal.

Some previously studied transition-metal dimer ions, such as $CoFe^+$,[5] VFe^+,[6] and $CuFe^+$,[7] have a reactivity that differs significantly from the reactivity of the corresponding atomic metal ions. For instance, VFe^+ is unreactive with linear and cyclic alkanes, while V^+ and Fe^+ activate C–C and C–H bonds in alkanes.[8,9] This is typical for clusters that are composed of first-row transition metals. $RhFe^+$, $RhCo^+$, and $LaFe^+$,[10] on the other hand, combine first- and second- or first- and third-row transition metals. These clusters exhibit reactivity similar to Fe^+,[4] Rh^+,[11] and La^+[12] in that they react with linear alkanes via C–C and C–H bond insertion mechanisms. The $MgFe^+$ dimer can also be considered a mixed-row cluster ion, but now a main-group metal is combined with a transition metal. Similar to the mixed-row transition-metal dimers, $MgFe^+$ reacts with alkanes, but mostly by C–H bond activation. $MgFe^+$ also exhibits some unique reactivity. This is the first example of both metals in a dimer reacting by displacement to sometimes generate an Fe^+–L product and other times to form a Mg^+–L product. This reactivity is due to a changeover in the relative metal–ligand bond energies when the ligand is an alcohol or an alkene. This paper will compare the chemistry of $MgFe^+$ with several previously characterized transition-metal dimer ions. In addition, a detailed theoretical treatment is provided to describe the bonding in $MgFe^+$ and an estimate of the Mg^+–Fe bond energy for comparison to experiment.

Experimental Section

Experiments were performed on a prototype Nicolet FTMS-1000 Fourier transform mass spectrometer[13] and a Nicolet FTMS-2000.[14] The FTMS-1000 is equipped with a 5.2-cm cubic trapping cell situated between the poles of a Varian 15-in. electromagnet maintained at 0.85 T. Mg^+ was generated by use of a pulsed Quanta Ray Nd:YAG laser (1064 nm) focused onto a magnesium target supported on the transmitter plate nearest the laser.[15] The FTMS-2000 is equipped with a differentially pumped dual cell situated in the bore of a superconducting magnet maintained at 3 T. For this study, the system was used as a single 4.8-cm cubic cell with all the experiments performed in the analyzer side. The Mg^+ was generated by use of laser desorption from a target placed in a four-way cross external to the magnetic field on the analyzer side of the instrument.

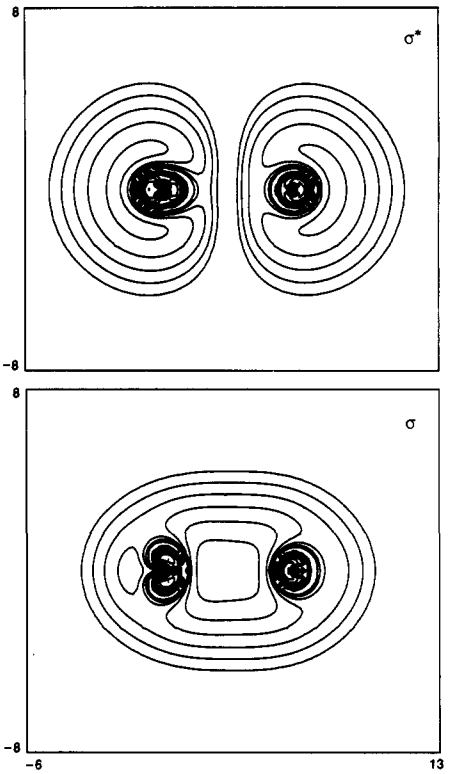

Figure 1. Log plot of the charge density for the σ and σ^* valence s orbitals. Fe is at the origin.

Chemicals were obtained in high purity from commercial sources and used as supplied except for multiple freeze–pump–thaw cycles to remove noncondensable gases. $Fe(CO)_5$ was introduced by a General Valve Corp. Series 9 pulsed solenoid valve.[16] This prevented subsequent reaction between the cluster ion and a background pressure of iron pentacarbonyl. Argon was used as the collision gas for collision-induced dissociation (CID) at a total pressure of $\simeq 5 \times 10^{-5}$ Torr (FTMS 1000) and $\simeq 3 \times 10^{-6}$ Torr (FTMS 2000). Uncalibrated Bayard–Alpert ionization gauges were used to monitor the static pressure.

Ion structures were investigated with use of collision-induced dissociation.[17] The translational energy of the ions was varied typically between 0 and 150 eV on the FTMS 1000 and 0 and 250 eV on the FTMS 2000. The spread in kinetic energy is approximately 35% at 1 eV, 10% at 10 eV, and 5% at 30 eV.[18] Photodissociation studies on $MgFe^+$ were performed on the FTMS 1000 by use of a 2.5-kW Hg–Xe arc lamp in conjunction with cutoff filters.

$MgFe^+$ was generated by use of a standard multipulse technique.[5] Specifically, Mg^+ was reacted with $Fe(CO)_5$ to form $MgFe(CO)_4^+$ exclusively, reaction 1. The remaining carbonyls were then stripped from the cluster by collision with argon, reaction 2. The bare metal cluster

$$Mg^+ + Fe(CO)_5 \rightarrow MgFe(CO)_4^+ + CO \quad (1)$$

$$MgFe(CO)_4^+ \xrightarrow{CID,\ Ar} MgFe^+ + 4CO \quad (2)$$

ion was isolated with use of swept double-resonance ejection pulses, trapped for 1 s in $\simeq 3 \times 10^{-6}$ Torr of argon to allow dissipation of excess energy by ~60 thermalizing collisions, and then reacted with a variety of organic samples. Linear pseudo-first-order decay plots were obtained for $MgFe^+$ reacting with *n*-heptane and cyclohexene ($2^1/_2$ half-lives), and product ion distributions were not affected significantly by varying the background Ar pressure. Both of these results suggest that the majority of the ions were thermalized. The presence of a small population of nonthermal ions, however, cannot be completely ruled out.

Ab Initio Calculations

Qualitative Considerations. The bonding in $MgFe^+$ is rather complex because several low-lying asymptotes contribute differ-

(2) Kumar, S.; Hanson, W. B. *J. Geophys. Res.* **1980**, *85*, 6783.
(3) (a) Operti, L.; Tews, E. C.; Freiser, B. S. *J. Am. Chem. Soc.* **1988**, *110*, 3847. (b) Operti, L.; Tews, E. C.; MacMahon, T. J.; Freiser, B. S. *J. Am. Chem. Soc.* **1989**, *111*, 9152. (c) Uppal, J. S.; Staley, R. H. *J. Am. Chem. Soc.* **1982**, *104*, 1229. (d) Rowe, B. R.; Fahey, D. W.; Ferguson, E. E.; Fehsenfeld, F. C. *J. Chem. Phys.* **1981**, *75*, 3325. (e) Po, P. L.; Porter, R. F. *J. Am. Chem. Soc.* **1977**, *99*, 4922.
(4) For example, see: (a) Jacobson, D. B.; Freiser, B. S. *J. Am. Chem. Soc.* **1983**, *105*, 5197. (b) Jacobson, D. B.; Freiser, B. S. *J. Am. Chem. Soc.* **1983**, *105*, 7484. (c) Jacobson, D. B.; Freiser, B. S. *J. Am. Chem. Soc.* **1983**, *105*, 7492. (d) Peake, D. A.; Gross, M. L.; Ridge, D. P. *J. Am. Chem. Soc.* **1984**, *106*, 4307. (e) Halle, L. F.; Armentrout, P. B.; Beauchamp, J. L. *Organometallics* **1982**, *1*, 963.
(5) Jacobson, D. B.; Freiser, B. S. *J. Am. Chem. Soc.* **1985**, *107*, 1581.
(6) Hettich, R. L.; Freiser, B. S. *J. Am. Chem. Soc.* **1985**, *107*, 6222.
(7) Tews, E. C.; Freiser, B. S. *J. Am. Chem. Soc.* **1987**, *109*, 4433.
(8) Jackson, T. C.; Carlin, T. J.; Freiser, B. S. *J. Am. Chem. Soc.* **1986**, *108*, 1120.
(9) Byrd, G. D.; Burnier, R. C.; Freiser, B. S. *J. Am. Chem. Soc.* **1982**, *104*, 3565.
(10) Huang, Y.; Buckner, S. W.; Freiser, B. S. In *Physics and Chemistry of Small Clusters*; Jena, P., Rao, B. K., Khanna, S. N., Eds.; Plenum: New York, 1987; p 891.
(11) Byrd, G. D.; Freiser, B. S. *J. Am. Chem. Soc.* **1982**, *104*, 5944.
(12) Wise, M. B.; Jacobson, D. B.; Huang, Y.; Freiser, B. S. *Organometallics* **1987**, *6*, 346.
(13) Buckner, S. W.; Gord, J. R.; Freiser, B. S. *J. Am. Chem. Soc.* **1988**, *110*, 6606.
(14) Gord, J. R.; Freiser, B. S. *Anal. Chim. Acta* **1989**, *225*, 11.
(15) Cody, R. B.; Burnier, R. C.; Reents, W. D., Jr.; Carlin, T. J.; McCrery, D. A.; Lengel, R. K.; Freiser, B. S. *Int. J. Mass Spectrom. Ion Phys.* **1980**, *33*, 37.
(16) Carlin, T. J.; Freiser, B. S. *Anal. Chem.* **1983**, *55*, 571.
(17) Cody, R. B.; Freiser, B. S. *Int. J. Mass Spectrom. Ion Phys.* **1982**, *41*, 199.
(18) Huntress, W. T.; Mosesman, M. M.; Elleman, D. D. *J. Chem. Phys.* **1971**, *54*, 843.

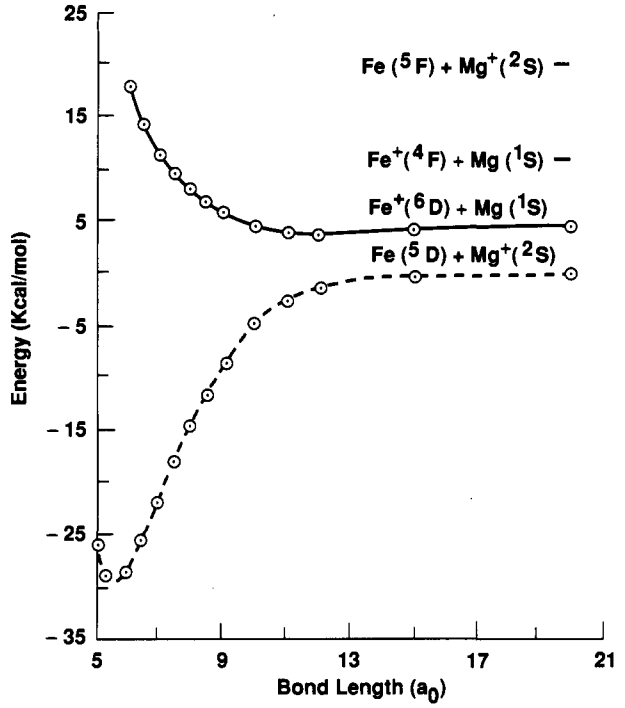

Figure 2. $X^6\Delta$ and $(2)^6\Delta$ states of $MgFe^+$. The higher asymptotes that give rise to the quartet states derived from the Fe and Fe^+ $3d^7$ occupations are also noted.

ently to the bonding. The lowest asymptote is $Mg^+ {}^2S(3s^1)$ + Fe $^5D(3d^64s^2)$, but the Mg $^1S(3s^2)$ + Fe^+ $^6D(3d^64s^1)$, Mg $^1S(3s^2)$ + Fe^+ $^4F(3d^7)$, and Mg^+ $^2S(3s^1)$ + Fe $^5F(3d^74s^1)$ asymptotes are only 5.2, 10.9, and 20.1 kcal/mol higher, respectively.[19] The most stable state is derived by mixing the two lowest asymptotes, leading to a $\sigma^2\sigma^{*1}$ valence s occupation. While this has a bond order of 0.5, the large polarizability of the metal atoms allows the antibonding orbital to polarize out of the bonding region so that the σ^* orbital becomes more nonbonding than antibonding,[20] Figure 1. The plot shows that the charge is nearly equally distributed on each atomic center. The Mulliken population analysis shows a charge on Fe of 0.51 electron, which is consistent with the orbital density plot. This bonding mechanism leads to one bound state and a repulsive state associated with a $\sigma^1\sigma^{*2}$ occupation, Figure 2. The three different high-spin occupations of the six Fe 3d electrons, when coupled with the two different occupations of the valence s electrons, lead to two $^6\Delta$, $^6\Pi$, and $^6\Sigma^+$ states. Since the Fe 3d electrons are not involved in the bonding, the three bound and three repulsive curves have virtually the same energy.

A bound quartet state can be formed by low-spin coupling the open-shell s electron to the 3d electrons. This state is higher in energy than the $X^6\Delta$ state due to the loss of exchange energy. However, quartet states also arise from the $Fe^+(3d^7)$ and Fe-$(3d^74s^1)$ asymptotes. Bonding from the Mg + $Fe^+(3d^7)$ asymptote requires Mg to donate electrons into the empty 4s orbital, while bonding from the Mg^+ + $Fe(3d^74s^1)$ asymptote involves forming a Mg(3s)–Fe(4s) bond. While these quartet states are derived from a higher asymptote, they are potentially low-lying as they have a bond order of 1.

Method of Calculation. The Fe basis set is derived from the (20s 12p 9d) basis set optimized by Partridge.[21] Three even-tempered 2p functions are added to describe the 4p orbital, an even-tempered diffuse 3d function is added to describe the $3d^74s^1$ occupation, and six even-tempered 4f functions are added for polarization. The even-tempered functions are of the form $\alpha = 2.5^n\alpha_0$, with $n = 0,\ldots, k$. The α_0(f) value is 0.1741. The Mg primitive set is the (20s 12p) set of Partridge[22] augmented with three p functions optimized for the ^3P state and supplemented with a 7d even-tempered set with $\alpha_0 = 0.0592$. These large primitive sets are contracted by use of the atomic natural orbital (ANO) procedure.[23] For Fe the average of the $^5D(3d^64s^2)$- and ^5F-$(3d^74s^1)$-state natural orbitals is used, while for Mg the average of the ^1S- and ^3P-state natural orbitals is used. The most diffuse s and p primitives are uncontracted to accurately describe the polarizability.[24] Our final contracted Gaussian basis sets are [7s 6p 4d 2f] and [6s 5p 2d] for Fe and Mg, respectively.

The self-consistent-field (SCF) approach is used to optimize the orbitals when the single reference-based modified coupled-pair functional approach[25] (MCPF) is used to include electron correlation and the state-averaged complete-active-space SCF (SA-CASSCF) approach is used for orbital optimization when external correlation is added by use of the multireference configuration-interaction (MRCI) method. The MRCI approach allows us to consider several states of the same symmetry and provides a valuable calibrant for the MCPF method. The smallest active space employed in the CASSCF treatment includes the Fe 3d and 4s and the Mg 3s orbitals and electrons. For the sextet states, this corresponds to a state-averaged SCF calculation. In this case, all configurations in the CASSCF are used as references in the subsequent MRCI calculation. The effect of higher excitations is accounted for by use of the multireference analogue of the Davidson correction (denoted +Q). The most important relativistic effects (+R) are accounted for by use of first-order perturbation theory.[26]

When only the Fe 3d and 4s electrons and Mg 3s electrons are included in the active space, the effect of the +Q correction on the $(2)^6\Delta$–$X^6\Delta$ separation is quite large, as the upper state is not as well-described as the ground state. Thus, we carried out calculations for the sextet states with the Fe 4p and Mg 3p orbitals included in the active space. As this greatly increases the size of the CASSCF wave function, reference selection was necessary; the reference lists for the MRCI treatment included all occupations for which the absolute value of the coefficient of any one of the component spin couplings exceeded 0.05 in the CASSCF wave function for r values between 5 and 20 a_0. Using this larger CASSCF/MRCI treatment greatly reduces the effect of the +Q corrections on the $(2)^6\Delta$–$X^6\Delta$ separation, yet the separation remains in excellent agreement with the smaller active-space calculations. Thus, the sextet calculations with the smaller active space should be reliable.

There is a large differential correlation contribution to the separation between states with different numbers of 3d electrons. This results in a large differential +Q correction when the quartet and sextet states are treated by use of the smaller active space. To reduce this differential +Q contribution, we expanded the CASSCF active space to include a 3d′ shell. In the subsequent MRCI calculations, we used a reference selection threshold of 0.025, which results in an expansion of nearly 3.8 million CSFs. At this level of treatment, the differential effect of higher excitations is small and the calculations are sufficiently reliable to accurately position the sextet and quartet manifolds.

All calculations were performed with use of the MOLECULE-SWEDEN program system.[27] In all calculations, only the pure spherical harmonic components of the basis functions are used.

Results

Unimolecular Chemistry of $MgFe^+$. Collision-induced dissociation on $MgFe^+$ results in the formation of both Fe^+ and Mg^+ as expected from their similar ionization potentials, IP(Mg) =

(19) Moore, C. E. *Atomic Energy Levels*; Circ 467; National Bureau Standards: Washington, DC, 1949.
(20) Bauschlicher, C. W., Jr.; Langhoff, S. R.; Taylor, P. R. *J. Chem. Phys.* **1988**, *88*, 1041.
(21) Partridge, H. *J. Chem. Phys.* **1989**, *90*, 1043.
(22) Partridge, H. *J. Chem. Phys.* **1987**, *87*, 6643.
(23) Almlof, J.; Taylor, P. R. *J. Chem. Phys.* **1987**, *86*, 4070.
(24) Bauschlicher, C. W., Jr. *Chem. Phys. Lett.* **1987**, *142*, 71.
(25) Chong, D. P.; Langhoff, S. R. *J. Chem. Phys.* **1986**, *84*, 5606. See also: Ahlrichs, R.; Scharf, P.; Ehrhardt, C. *J. Chem. Phys.* **1985**, *82*, 890.
(26) Martin, R. L. *J. Phys. Chem.* **1983**, *87*, 750 and references therein.
(27) MOLECULE-SWEDEN is an electronic structure program system written by J. Almlof, C. W. Bauschlicher, Jr., M. R. A. Blomberg, D. P. Chong, A. Heiberg, S. R. Langhoff, P.-A. Malmqvist, A. P. Rendell, B. O. Roos, P. E. M. Siegbahn, and P. R. Taylor.

Table I. Spectroscopic Constants for $MgFe^+$ (Fe Asymptote from which the $^4\Pi$ States Are Derived Is Denoted. All Entries Include a Correction (+R) for Relativistic Effects)

state	method	r_e (Å)	ω_e (cm^{-1})	D_0 (kcal/mol)	T_e (kcal/mol)
$X^6\Delta$	MRCI+Q	2.97	195	29.4	0.00
$A^6\Pi$	MRCI+Q	2.93	189	29.3	0.12
$(2)^6\Delta^a$	MRCI+Q				50.75
$^4\Pi(3d^6)$	MRCI+Q	2.96	170	21.0	8.39
$(2)^4\Pi(3d^7)^b$	MRCI+Q				9.34
$X^6\Delta$	MCPF	2.97	198		0.00
$^4\Delta(3d^7)$	MCPF	2.66	229		11.87
$^4\Pi(3d^7)$	MCPF	2.65	219		12.92

[a] This state is repulsive so that the T_e value corresponds to the vertical excitation energy. [b] Computed by use of the larger active-space MRCI treatment at the smaller active-space MRCI minimum.

7.646 eV and IP(Fe) = 7.87 eV.[28] At the lower CID energies, Mg^+ dominates in accordance with Stevenson's rule,[29] whereby the charge is retained by the fragment with the lower ionization potential. As the energy is increased, the relative intensities of the product ions approach each other as expected. In contrast, photodissociation yields predominantly Fe^+ (>95%) with only a small amount of Mg^+ formed over the wavelength range monitored (roughly 340–820 nm). These results are supported by theory as discussed in the following text.

The longest wavelength at which photodissociation occurs, or the photodissociation threshold, yields an upper limit on the bond dissociation energy. In many cases involving metal ion systems, however, the photodissociation threshold has been found to provide a good estimate of the absolute bond energy[30] because a high density of allowed electronic states exists in this energy region. However, if the first allowed electronic state lies at an energy above the thermodynamic bond energy, the photodissociation threshold is spectroscopically determined and can only be used to set an upper limit on the bond energy.[30] The threshold for the production of Fe^+ yields $D°(Fe^+–Mg) \leq 49$ kcal/mol, which in turn indicates $D°(Mg^+–Fe) \leq 44$ kcal/mol. Bond energy information was also obtained by use of ion–molecule reaction bracketing techniques. Specifically, $MgFe^+$ reacts with ethylene by displacement of magnesium to form $FeC_2H_4^+$, indicating $D°(Fe^+–Mg) < D°(Fe^+–C_2H_4) = 39 \pm 5$ kcal/mol[31] from which $D°(Mg^+–Fe) < 34 \pm 5$ kcal/mol is derived. The discrepancy between the bond energy values obtained from photodissociation and bracketing techniques suggests that, unfortunately, the photodissociation threshold is spectroscopic and not thermodynamic. This is one of the weakest bond energies reported for heteronuclear metal dimer ions, which thus far have ranged from 48 ± 5 kcal/mol for $LaFe^+$[32] and $ScFe^+$[33] to 75 ± 5 kcal/mol for VFe^+.[6]

Theoretical Treatment. Spectroscopic constants for the low-lying states of $MgFe^+$ are summarized in Table I. All values include the +R correction, and the MRCI results include the +Q correction. As expected, the $^6\Pi$ state is only slightly higher in energy (0.12 kcal/mol). Since the bonding in the $^6\Delta$ and $^6\Pi$ states is similar, higher levels of theory will not reverse the order of these two states. Therefore, the ground state is unquestionably the $X^6\Delta$ state. The binding energy (D_0) is computed to be 29.4 kcal/mol, in good agreement with the experimental upper limit of 34 ± 5 kcal/mol deduced from the ion–molecule reactions. Improvements in both the basis set and the correlation treatment are expected to increase the calculated D_0; thus, the theoretical value is a lower bound. Previous experience leads us to estimate that the computed result is accurate to ~5 kcal/mol. The $(2)^6\Delta–X^6\Delta$ vertical excitation energy is 50.8 kcal/mol. As the second $^6\Pi$ and $^6\Sigma^+$ states are slightly higher in energy, this represents the smallest excitation energy for photodissociation. Further, the transition moment is very large (>1 au), and hence, the absorption to this excited state and subsequent dissociation to $Fe^+ + Mg$ is what is observed in experiment at a photon energy of 49 kcal/mol. Thus, both the computed binding energy and excitation energy are in excellent agreement with experiment.

The populations indicate that the charge is nearly equally distributed on the Fe and Mg atoms for both states up to a bond length of more than 9 a_0. At larger r values, the charge begins to localize; by 11 a_0, the charge for the $X^6\Delta$ state is ~70% on Mg atom. Thus, it is only at long range where the lower IP of Mg results in the charge being localized on Mg atom.

The lowest quartet states are derived from the $3d^6$ occupation of Fe and Fe^+ and differ from the sextet states by having a low-spin coupling of the valence s and 3d shell. As with the sextet states, the 3d electrons are not involved in the bonding, and hence, all of the quartet states derived from this bonding mechanism have similar energies. The $^4\Pi$ state is found to be 8.4 kcal/mol above the $^6\Delta$ state at the MRCI+Q+R level. This is less than the 23.8 kcal/mol for the similar change in spin coupling in Fe^+, i.e., the $^6D(3d^64s^1)–^4D(3d^64s^1)$ separation.[19] The separation is smaller because the electron spends only half its time on Fe and the σ^* orbital polarizes away from Fe to reduce its impact on the bonding σ orbital. The bond length and vibrational frequencies are similar for the $^4\Pi$ and $^6\Delta$ states, and the spectroscopic constants are not strongly affected by the level of treatment.

The loss of exchange energy guarantees that the quartet states derived from the $3d^6$ occupations of Fe and Fe^+ must be above the sextet states with the same occupation. Therefore, if $MgFe^+$ were to have a quartet ground state, it must be derived from a $3d^7$ occupation. When the $3d^7$-derived states are treated at the MRCI level with use of the smaller active space, they are ~10 kcal/mol above the $3d^6$-derived quartet states but become slightly lower when the +R and +Q corrections are added. However, the very large differential +Q contribution is an artifact of the smaller active space, as it is reduced to only 1.6 kcal/mol when the larger active space is employed. Thus, our calculations are not sufficiently accurate to definitively determine whether the lowest quartet state is derived from the $3d^6$ or $3d^7$ Fe occupation, but since the quartet states lie ~10 kcal/mol above the ground state, the calculations rule out the possibility of a quartet ground state.

While the larger active-space calculations are more accurate, they are also very costly, requiring more than 10 h of CRAY YMP time for each geometry. Thus, no geometry optimizations were carried out at this level of theory. One obvious trend is that states derived from the $3d^7$ asymptote have shorter bond lengths than states derived from $3d^6$ asymptotes. This is due to the higher bond order for states derived from $3d^7$. As for the $3d^6$-derived states, the $^4\Delta$ and $^4\Pi$ states derived from the $3d^7$ occupation have very similar energies. At the MCPF level, these states differ by only ≃1 kcal/mol and have very similar spectroscopic constants, Table I. At the MRCI+Q+R level, the $^4\Pi$ state derived from the $3d^6$ asymptote lies ≃1 kcal/mol below the $^4\Pi$ state derived from the $3d^6$ asymptote. The separation between the sextet and quartet manifolds is found to be slightly larger at the MCPF+R level than at the MRCI+Q+R level. Even though higher levels of correlation treatment may further favor the quartet states, we are confident that the ground state of $MgFe^+$ is $X^6\Delta$.

Reactions with Alkanes. $MgFe^+$ is unreactive with ethane, propane, butane, and neopentane, Table II. However, it does activate C–H bonds in *n*-pentane to eliminate H_2 and form $MgFeC_5H_{10}^+$, reaction 3. This product reacts further with *n*-pentane under extreme conditions (6-s reaction time and pentane pressure of 2×10^{-6} Torr) to displace magnesium and dehydrogenate the ligand to form $Fe(C_5H_{10})_2^+$, reaction 4. The neutral

$$MgFe^+ + n\text{-}C_5H_{12} \xrightarrow{100\%} MgFeC_5H_{10}^+ + H_2 \quad (3)$$

$$MgFeC_5H_{10}^+ + n\text{-}C_5H_{12} \xrightarrow{100\%} Fe(C_5H_{10})_2^+ + (MgH_2) \quad (4)$$

(28) Lias, S. G.; Bartmess, J. E.; Liebman, J. F.; Holmes, J. L.; Levin, R. D.; Mallard, W. G. *J. Phys. Chem. Ref. Data, Suppl. 1* **1988**, *17*.
(29) Harrison, A. G.; Finney, C. D.; Sherk, J. A. *Org. Mass Spectrom.* **1971**, *5*, 1313.
(30) Hettich, R. L.; Jackson, T. C.; Stanko, E. M.; Freiser, B. S. *J. Am. Chem. Soc.* **1986**, *108*, 5086.
(31) van Koppen, P. A. M.; Bowers, M. T.; Beauchamp, J. L.; Dearden, D. V. *Bonding Energetics in Organometallic Compounds*; Marks, T. J., Ed.; *ACS Symp. Ser.* **1990**, *No. 428*, 34.
(32) Huang, Y.; Freiser, B. S. *J. Am. Chem. Soc.* **1988**, *110*, 387.
(33) Hettich, R. L.; Freiser, B. S. *J. Am. Chem. Soc.* **1987**, *109*, 3537.

Table II. Distribution of the Primary and Secondary Products of $MgFe^+$

reagent	neutral loss	primary product	rel %	neutral loss	secondary[a] product	rel %
ethane		NR				
propane		NR				
butane		NR				
n-pentane	H_2	$MgFeC_5H_{10}^+$	100	Mg, H_2	$Fe(C_5H_{10})_2^+$	100
n-hexane	H_2	$MgFeC_6H_{12}^+$	100	$3H_2$	$MgFeC_6H_6^+$[b]	100
n-heptane	H_2	$MgFeC_7H_{14}^+$	56			
	Mg, H_2	$FeC_7H_{14}^+$	27			
	Mg	$FeC_7H_{16}^+$	17			
cyclopropane		NR				
cyclobutane		NR				
cyclopentane	$2H_2$	$MgFeC_5H_6^+$	100	Mg, $3H_2$	$Fe(C_5H_5)_2^+$	100
cyclohexane	$2H_2$	$MgFeC_6H_8^+$	35			
	$3H_2$	$MgFeC_6H_6^+$	65			
ethylene	Mg	$FeC_2H_4^+$	100			
propene	Mg	$FeC_3H_6^+$	100			
cis-2-butene	H_2	$MgFeC_4H_6^+$	19	Mg	$FeC_8H_{14}^+$	100
	Mg	$FeC_4H_8^+$	81			
trans-2-butene	H_2	$MgFeC_4H_6^+$	27	Mg	$FeC_8H_{14}^+$	100
	Mg	$FeC_4H_8^+$	73			
isobutene	Mg	$FeC_4H_8^+$	100			
1-pentene	Mg	$FeC_5H_{10}^+$	100			
1-hexene	Mg	$FeC_6H_{12}^+$	100			
cyclopentene	H_2	$MgFeC_5H_6^+$	72	Mg, $2H_2$	$Fe(C_5H_5)_2^+$	100
	Mg	$FeC_5H_8^+$	28			
cyclohexene	$2H_2$	$MgFeC_6H_6^+$	68	Mg	C_6H_6–Fe^+–C_6H_{10}	100
	Mg, $2H_2$	$FeC_6H_6^+$	32			
cycloheptene	Mg, $2H_2$	$FeC_7H_8^+$	45			
	$2H_2$	$MgFeC_7H_8^+$	55	Mg	C_7H_{12}–Fe^+–$C_7H_8^+$	100
water		NR				
methanol	Fe	$MgCH_3OH^+$	100			
ethanol	Fe	$MgC_2H_5OH^+$	100			
2-propanol	Fe	$MgC_3H_7OH^+$	100			
2-butanol	Fe	$MgC_4H_9OH^+$	100			
acetone	Fe	Mg–acetone$^+$	100			

[a] Secondary reactions are reported only for $MgFeL^+$ because the reactions of FeL^+ and MgL^+ have been previously reported. [b] From thermal CID.

lost from reaction 4 may be either Mg + H_2 or MgH_2. While the loss of FeH_2 is at least 22 kcal/mol more exothermic than the loss of Fe and H_2,[34] the loss of Mg and H_2 is only $\simeq$3 kcal/mol more exothermic than the loss of MgH_2.[35] Thus, the formation of either neutral product is possible and will be indicated by (MgH_2) in the remainder of the paper. It is interesting that in $MgFeL^+$ the first ligand forms an Fe^+–L bond that is stronger than the metal–metal bond, so that the secondary reaction results in the elimination of magnesium. This effect is further supported by CID of $MgFeC_5H_{10}^+$, which, at low energies, results in the loss of magnesium to form $FeC_5H_{10}^+$. As the CID energy is increased, $FeC_5H_{10}^+$ is observed to fragment by loss of ethylene, propene, and methane as has been previously reported.[4a]

$MgFe^+$ also reacts with *n*-hexane initially by dehydrogenation to form $MgFeC_6H_{12}^+$, reaction 5. Interestingly, at longer trapping times this species is observed to yield $MgFeC_6H_6^+$. Increasing the background pressure of hexane or introducing argon enhances this reaction. This unusual behavior has been previously observed for $CoC_3H_7^+$ which, in the presence of either propane or argon as the neutral gas, forms $CoC_3H_5^+$.[36] Apparently, the $MgFeC_6H_{12}^+$ generated in reaction 5 is formed with an internal energy very near that required for further dehydrogenation. A thermal CID process then results in dehydrogenation of the $MgFeC_6H_{12}^+$ to presumably form $MgFe^+$–benzene, reaction 6.

$$MgFe^+ + n\text{-}C_6H_{14} \xrightarrow{100\%} MgFeC_6H_{12}^+ + H_2 \quad (5)$$

$$MgFeC_6H_{12}^{+*} \xrightarrow{100\%} MgFeC_6H_6^+ + 3H_2 \quad (6)$$

Dehydrocyclization has also been observed in several instances. $CoFe^+$, for example, reacts with 1-hexene to form $CoFeC_6H_{10}^+$ and $CoFeC_6H_8^+$, which, upon CID, results in facile dehydrocyclization to form $CoFe^+$–benzene.[5] In addition, the mixed-row transition-metal dimer ions (which combine a first- and second- or a first- and third-row transition metal) also initiate dehydrocyclization. $LaFe^+$ reacts with *n*-hexane to dehydrogenate the ligand. The resulting ion eliminates H_2 upon CID to form a dimer–benzene ion.[32] In fact, $RhFe^+$[10] and $NbFe^+$[37] react with *n*-hexane and 1-hexene, respectively, to form the dimer–benzene ion directly. This reaction, therefore, illustrates the similarity between $MgFe^+$ and the previously studied mixed-row transition-metal cluster ions.

$MgFe^+$ reacts with *n*-heptane to form three products, reactions 7–9, with no secondary reactions observed. Once again, dehydrogenation is the major reaction pathway forming $MgFeC_7H_{14}^+$.

$$MgFe^+ + n\text{-}C_7H_{16} \xrightarrow{56\%} MgFeC_7H_{14}^+ + H_2 \quad (7)$$

$$\xrightarrow{27\%} FeC_7H_{14}^+ + (MgH_2) \quad (8)$$

$$\xrightarrow{17\%} FeC_7H_{16}^+ + Mg \quad (9)$$

CID of this ion resulted in loss of magnesium at low energies. As the CID energy increased, both the elimination of magnesium and losses corresponding to C_2H_4, C_2H_6 or $C_2H_4 + H_2$, C_3H_6, C_3H_8 or $C_3H_6 + H_2$, C_4H_8, and C_5H_{10} are observed. CID of $FeC_7H_{14}^+$ from reaction 8 yields predominantly the loss of C_3H_6 and $C_3H_6 + H_2$ to form $Fe(C_4H_8)^+$ and $Fe(C_4H_6)^+$ at low energies, and at higher energies, loss of C_4H_8 to form $Fe(C_3H_6)^+$ is also observed. The CID results of $FeC_7H_{14}^+$ from reaction 8 suggest, although not conclusively, a propene–butene structure.[4a] Furthermore, the additional losses of C_2H_4, C_2H_6, and C_5H_{10} observed at higher energies from $MgFeC_7H_{14}^+$ indicate the presence of a second isomer of $FeC_7H_{14}^+$, namely the ethene–pentene species. This mixture of at least two isomers probably occurs during the CID activation step rather than initially in reaction 7. An earlier study failed to distinguish the bisolefin isomers from the monoolefin

(34) Halle, L. F.; Klein, F. S.; Beauchamp, J. L. *J. Am. Chem. Soc.* **1984**, *106*, 2543.
(35) Pople, J. A.; Luke, B. T.; Frisch, M. J.; Binkley, J. S. *J. Phys. Chem.* **1985**, *89*, 2198.
(36) Jacobson, D. B.; Freiser, B. S. *J. Am. Chem. Soc.* **1984**, *106*, 3891.
(37) Buckner, S. W.; Freiser, B. S. *J. Phys. Chem.* **1989**, *93*, 3667.

(heptene) $FeC_7H_{14}^+$ isomers due to facile rearrangement of the monoolefin and bisolefin products.[4a] The third product is formed by the displacement of magnesium to yield $FeC_7H_{16}^+$, reaction 9. This process is not observed for any of the other MFe^+ species previously studied and once again is indicative of the weak Fe^+–Mg bond. The formation of Fe^+–alkane species has been previously observed by Ridge and co-workers in a high-pressure ion source containing $Fe(CO)_5$ and an alkane. They postulated a ligand displacement reaction with Fe^+–CO to form Fe^+–alkane.[38] The $MgFe^+$ product is formed by a similar process. CID of this product was attempted, but the ion proved impossible to isolate and dissociate. Once again, the addition of a ligand to the cluster ion forms an Fe^+–L bond that is stronger than the metal–metal bond.

$MgFe^+$ is unreactive with cyclopropane and cyclobutane. It does, however, react with cyclopentane to form presumably $MgFe^+$–cyclopentadiene. A secondary product, the ferrocenium ion, is observed at long reaction times (≥10 s) and at high pressures of cyclopentane (≃10^{-6} Torr). This stable ion is formed by displacement of Mg and further dehydrogenation of the ligands. $MgFe^+$ also reacts with cyclohexane to form the two dehydrogenation products $MgFe^+$–cyclohexadiene and $MgFe^+$–benzene, reactions 10 and 11. No secondary reactions were observed. CID

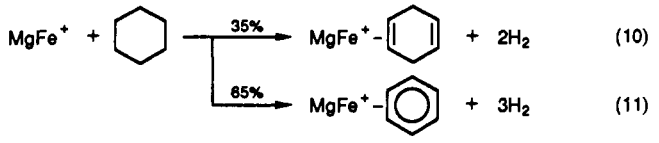

of the $MgFe^+$–cyclohexadiene yields $MgFe^+$–benzene by dehydrogenation. This ion (from both the CID process and reaction 11) loses magnesium to form Fe^+–benzene and, at higher energies, loses the ligand and magnesium to form Fe^+. These results are consistent with a $MgFe^+$–benzene structure.

Reactions with Linear Alkenes. The reactions of $MgFe^+$ with alkenes ranging from ethylene to 1-hexene were studied. In general, $MgFe^+$ reacts with linear alkenes by displacement of magnesium to form an Fe^+–alkene structure as the primary product, reaction 12. The Fe^+–alkene product ion then undergoes

$$MgFe^+ + \text{linear alkene} \rightarrow Fe^+\text{–(alkene)} + Mg \quad (12)$$

secondary reactions with the background alkene as has been previously reported.[4b]

Two primary products are formed in the reaction between $MgFe^+$ and *cis*-2-butene and *trans*-2-butene, reactions 13 and 14.

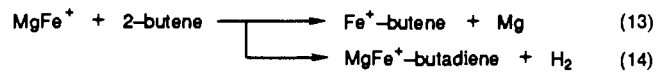

As expected, Fe^+–butene is a product. However, $MgFe^+$–butadiene also forms. This reaction is interesting because it is the only example of the $MgFe^+$ cluster remaining intact while reacting with a linear alkene. CID of $MgFeC_4H_6^+$ results in the loss of magnesium to form Fe^+–butadiene. This is in agreement with the evidence for a weak $MgFe^+$ bond ($D°(Fe^+–Mg) < D°(Fe^+–butadiene) = 48 \pm 5$ kcal/mol).[30] At higher energies, Fe^+ is formed by loss of the intact ligand and magnesium. A third product, $Fe^+–C_4H_6$, is also formed in low abundance. However, this is an endothermic reaction product that provides an unrealistic upper limit of 19 kcal/mol for $D°(Fe^+–Mg)$ by use of $D°(Fe^+–C_4H_6) = 48 \pm 5$ kcal/mol.[30] This product could be due to a small population of nonthermal ions.

$MgFe^+$ reacts with 1-pentene to form $FeC_5H_{10}^+$. CID of this species results in the loss of ethylene, propene, and methane, which are the same as the CID products from Fe(1-pentene)$^+$ generated from the reaction of Fe^+ with *n*-heptane reported earlier.[4a] $MgFe^+$ reacts with 1-hexene to yield $FeC_6H_{12}^+$, exclusively. The CID of this product is consistent with the CID of Fe(1-hexene)$^+$ formed from linear alkanes larger than heptane. Losses of C_2H_4, C_2H_6 or $C_2H_4 + H_2$, and C_3H_6 are observed.[4a] A secondary reaction is also observed with the condensation of another alkene onto the existing ion in addition to the displacement of C_3H_6 by C_6H_{12}.

Reactions with Cyclic Alkenes. $MgFe^+$ also reacts with C_5–C_7 cyclic alkenes. The dimer reacts with cyclopentene to form $MgFe^+$–cyclopentadiene and Fe^+–cyclopentene, reactions 15 and 16. Double-resonance ion-ejection experiments reveal that the majority of the secondary product, ferrocenium ion, is formed from $MgFeC_5H_6^+$, reaction 17. While $FeC_5H_8^+$ also reacts with

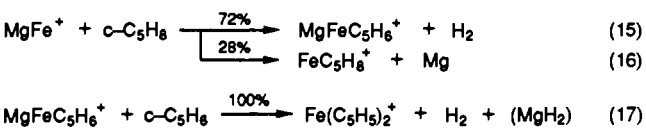

cyclopentene to form ferrocenium, the reaction rate is slower. The dimer also reacts with cyclohexene to form $MgFe^+$–benzene and Fe^+–benzene as the primary products, reactions 18 and 19. Assuming that the neutral products in reaction 19 are Mg + $2H_2$ and that the reaction is exothermic, and by use of $D°(Fe^+–C_6H_6) = 55 \pm 5$ kcal/mol,[30] a $D°(Fe^+–Mg) \leq 34 \pm 5$ kcal/mol is calculated, which in turn yields $D°(Mg^+–Fe) \leq 29 \pm 5$ kcal/mol. While these limits are 5 kcal/mol lower than those determined from reaction 12 with ethylene, due to the uncertainty of the neutral products in reaction 19, the more conservative limits obtained from ethylene hold greater confidence. A secondary product is also observed that corresponds to benzene–Fe^+–cyclohexene. This ion arises both from $MgFe^+$–benzene, reaction 20, and from Fe^+–benzene as reported previously.[4c] Analogous results were obtained with cycloheptene.

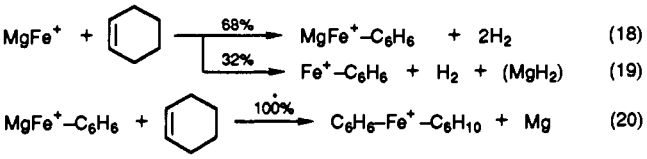

Reactions with Oxygen-Containing Compounds. $MgFe^+$ reacts with methanol, ethanol, 2-propanol, and 2-butanol to displace the iron and form a Mg^+–alcohol product. For example, $MgFe^+$ reacts with ethanol to form $MgC_2H_5OH^+$, reaction 21. This reaction

$$MgFe^+ + C_2H_5OH \xrightarrow{100\%} MgC_2H_5OH^+ + Fe \quad (21)$$

was expected to occur due to the high bond energy of $Mg^+–C_2H_5OH$ (63 ± 5 kcal/mol[3a]). A secondary product corresponding to $Mg(C_2H_5OH)_2^+$ was also observed, as reported in a previous study on Mg^+.[3a] In a similar manner, acetone reacts with $MgFe^+$ to form Mg^+–acetone as the primary product, reaction 22. CID of this ion results in loss of the intact ligand to form Mg^+. A secondary product forms slowly by condensation of a second acetone molecule to yield $Mg(acetone)_2^+$.

$$MgFe^+ + \text{acetone} \xrightarrow{100\%} Mg^+\text{–acetone} + Fe \quad (22)$$

Surprisingly, no reaction was observed to occur between $MgFe^+$ and H_2O. Displacement of Fe to form MgH_2O^+ was expected to occur because an extrapolated value of $D°(Mg^+–H_2O)$ of 60 ± 5 kcal/mol has been reported.[3b] However, this result is consistent with a recent theoretical value of $D°(Mg^+–H_2O) \leq 36 \pm 5$ kcal/mol.[39] Finally, absence of reaction with water to form FeH_2O^+ is consistent with $D°(Fe^+–Mg) > D°(Fe^+–H_2O) = 32 \pm 2$ kcal/mol.[40]

Discussion

$MgFe^+$ has a weak Mg^+–Fe bond energy (≤34 ± 5 kcal/mol) when compared to the other transition-metal dimer ions, which has a dramatic effect on its chemistry. The majority of diatomic transition-metal cluster ions are not reactive with alkanes. This

(38) Larsen, B. S.; Ridge, D. P. *J. Am. Chem. Soc.* **1984**, *106*, 1912.

(39) Bauschlicher, C. W., Jr.; Partridge, H. *J. Phys. Chem.*, in press.

(40) (a) Rosi, M.; Bauschlicher, C. W., Jr. *J. Chem. Phys.* **1990**, *92*, 1876. (b) Marinelli, P. J.; Squires, R. R. *J. Am. Chem. Soc.* **1989**, *111*, 4101. (c) Magnera, T. F.; David, D. E.; Michl, J. *J. Am. Chem. Soc.* **1989**, *111*, 4100.

is in sharp contrast to the reactivity of the atomic transition-metal ions with alkanes where both C–C and C–H bond insertion are observed. Only mixed-row transition-metal dimers, such as $LaFe^+$, $RhFe^+$, and $RhCo^+$,[10] have exhibited both C–H and C–C bond insertion. It is postulated that this reactivity is due to reduced orbital overlap between the metals present in the dimer. This would allow the constituents of the dimer to have more atomic character. In comparison, $MgFe^+$ inserts into C–H bonds in alkanes; however, activation of C–C bonds was not observed. A similar explanation could account for the reactivity of $MgFe^+$. The combination of a first-row transition metal and a main-group element could result in poor orbital overlap and a reactivity reminiscent of Fe^+.

For example, both $MgFe^+$ and Fe^+ are unreactive with methane and ethane. However, commencing with propane, Fe^+ activates both C–C and C–H bonds to eliminate small alkanes and H_2, respectively.[4a] $MgFe^+$, likewise, dehydrogenates alkanes larger than *n*-pentane. However, initial C–C bond insertion is absent. An interesting reaction occurs between $MgFe^+$ and *n*-hexane. Initially, the dimer dehydrogenates the hexane to form $MgFeC_6H_{12}^+$. However, this species must have an internal energy near the threshold for further dehydrogenation because, at longer times, $MgFeC_6H_{12}^{+*}$ forms $MgFeC_6H_6^+$. This effect is enhanced by increasing the pressure of the neutral gases. A thermal CID process must be occurring.

The chemistries of $MgFe^+$ and Fe^+ are more similar for cyclic alkanes. Both ions are unreactive with cyclopropane but dehydrogenate cyclopentane and cyclohexane.[4c] In fact, the only difference is the extent of dehydrogenation. Fe^+ reacts with cyclopentane to form Fe^+–cyclopentene (77%) and Fe^+–cyclopentadiene (23%),[4c] while $MgFe^+$ reacts to form $MgFe^+$–cyclopentadiene, exclusively. In addition, Fe^+ reacts with cyclohexane to eliminate H_2 (55%), $2H_2$ (24%), and $3H_2$ (21%).[4c] $MgFe^+$, however, only forms two products: $MgFe^+$–cyclohexadiene and $MgFe^+$–benzene. No single dehydrogenation is observed in the reaction with the dimer ion.

The effect of the weak $MgFe^+$ bond energy is also evident in the reaction with linear alkenes, where the magnesium is displaced in the primary reaction to form Fe^+–alkene. In fact, $MgFe^+$ reacts with both ethylene and propene. Previously, all of the heteronuclear transition-metal diatomic clusters were unreactive with propene and ethylene. The only exception was $NbFe^+$, which was observed to react with propene to form $NbFeC_3H_4^+$.[37]

The reaction of $MgFe^+$ with cyclic alkenes (for example, cyclohexene) is also similar to several previously studied metal cluster ions. For instance, $CoFe^+$ dehydrogenates cyclohexene to form a dimer–benzene ion. In addition, $CoC_6H_6^+$ is also generated.[5] This is similar to the reactivity of $MgFe^+$, except that Fe is displaced in the $CoFe^+$. While $NbFe^+$ initially forms a dimer–benzene product, the secondary reaction displaces Fe and forms Nb^+–$C_{12}H_{12}$[37] which, again, is reminiscent of the reactivity of $MgFe^+$. However, for $MgFe^+$, the secondary reaction product is the simple displacement of Mg by cyclohexene to form a cyclohexene–Fe^+–benzene species. This differs from the previously characterized metal dimer ions that dehydrogenated the additional ligand to form a bisbenzene species.[37,41] However, this product is similar to the secondary reactions of Fe^+–benzene with cyclohexene, which form both C_6H_{10}–Fe^+–C_6H_6 and C_6H_8–Fe^+–C_6H_6.[4c] Other parallels exist for cyclopentene and cycloheptene.

$MgFe^+$ is the first transition-metal dimer ion that exhibits a changeover in relative metal–ligand bond energies. In addition to its reactivity with linear alkenes to displace magnesium and form Fe^+–alkene species, $MgFe^+$ also reacts with alcohols to displace iron and form Mg^+–alcohol species.

Acknowledgment is made to the Division of Chemical Sciences in the Office of Basic Energy Sciences in the U.S. Department of Energy (Grant DE-FG02-87ER13766) for supporting this research and to the National Science Foundation (Grant CHE-8920085) for continued support of the FTMS.

Registry No. $FeMg^+$, 132338-93-3; ethane, 74-84-0; propane, 74-98-6; butane, 106-97-8; neopentane, 463-82-1; cyclopropane, 75-19-4; cyclobutane, 287-23-0; *n*-pentane, 109-66-0; *n*-hexane, 110-54-3; *n*-heptane, 142-82-5; cyclopentane, 287-92-3; cyclohexane, 110-82-7; ethylene, 74-85-1; propene, 115-07-1; *cis*-2-butene, 590-18-1; *trans*-2-butene, 624-64-6; isobutene, 115-11-7; 1-pentene, 109-67-1; 1-hexene, 592-41-6; cyclopentene, 142-29-0; cyclohexene, 110-83-8; cycloheptane, 628-92-2; water, 7732-18-5; methanol, 67-56-1; ethanol, 64-17-5; 2-propanol, 67-63-0; 2-butanol, 78-92-2; acetone, 67-64-1.

(41) Lech, L. M.; Gord, J. R.; Freiser, B. S. *J. Am. Chem. Soc.* **1989**, *111*, 8588.